Comparison of Magnetic Noise Compensation Techniques for Dual Three-Phase Electrically Excited Synchronous Machines

Jonas Henkenjohann, Jan Andresen*, Axel Mertens
Leibniz University Hannover
Institute for Drive Systems and Power Electronics
Welfengarten 1
Hannover, Germany
Phone: +49 (0) 511 762 5619
Fax: + 49 (0) 511 762 3040
Email: jonas.henkenjohann@ial.uni-hannover.de
URL: https://www.ial.uni-hannover.de/

Acknowledgments

This work is part of the project *DampedWEA* and was funded by the Federal Ministry for Economic Affairs and Climate Action on the basis of a decision by the German Bundestag. Funding number: 03EE2008D. The authors would like to thank the industrial project partner Enercon for the inspiration to compare HFI and FFI when applied to an EESM, and the continuous support during the process.

Keywords

≪Force Control≫, ≪Acoustic noise≫, ≪Multiphase drive≫, ≪Vibration suppression≫

Abstract

This paper presents a detailed comparison of two commonly known magnetic noise compensation methods. One is based on forces generated by harmonic currents interacting with the fundamental field, while the other uses a harmonic field. Both methods are applied to dual three-phase electrically excited synchronous machines. The required compensation currents and parasitic effects, such as the induced voltage in the field winding, are compared. Furthermore, known precalculation methods are adapted to dual three-phase electrically excited synchronous machines and validated with FEM calculations.

Introduction

The ever-increasing number of electrical machines permeating more and more aspects of human life is leading to increased attention regarding the noise which they generate. Particularly due to the transformation of the energy system and the associated increase in the use of synchronous electrical machines in applications with a high power density (e.g., wind energy and traction drives), multiphase machines are now a strong focus of noise-reduction research. As [1] describes, electrically excited synchronous machines (EESM) offer various advantages over permanent magnet synchronous machines (PMSM). For example, the implementation of field weakening is easier, rare-earth magnets are not required and irreversible demagnetisation of an EESM cannot occur.

The noise emissions of electrical machines is often dominated by the radial mode 0 [2]. For this reason, there are already a large number of approaches in the literature for influencing the noise behaviour of electrical drives by injecting harmonic currents to compensate for the electromagnetic force excitation

*Now with: KEB Automation KG, Südstraße 38, Barntrup, Germany

of mode 0. In [3–7], optimal harmonic currents are determined with the help of parameter variations and numerical simulations. However, these methods are computationally intensive.

To overcome this issue, precalculation methods based on the rotating field theory have also been developed in the literature [8–10]. However, these methods neglect the tangential field component and for this reason are not able to predict the tangential tensile stresses within the machine. In [11], the analytical relationships for a PMSM are derived to enable the calculation of both the radial and tangential tensile stresses that result from injecting an additional spatial fundamental harmonic field. In this work, this is referred to as fundamental field injection (FFI). In a second step, the analytical relationships can be used to calculate the harmonic currents needed for compensation. In [12], the knowledge gained is validated on a test bench. Similar predictions of valid noise compensating currents for EESMs have not yet been documented in the literature.

This paper extends the analytical methods from [11] to include dual three-phase EESMs and evaluates the additional degrees of freedom that arise when applying for the FFI method. As a second approach, the investigations of dual three-phase PMSMs in [3], which have shown that compensation of the radial mode 0 can also be achieved by injecting spatial harmonic fields, are also examined within the scope of this work. This procedure is called harmonic field injection (HFI) in the following text. This paper derives an analytical equation relating tensile stress to harmonic current, so that computation intensive parameter variations as reported in [3] can be avoided for the HFI method.

Noise compensation in three-phase machines

This paper builds on the work of [11], uses the same notation, and adopts the consideration of the air-gap field as a sum of individual rotating waves. Since the machine under investigation is a synchronous machine, the dependence on time is replaced by the angular rotor position in this paper. The air-gap field can thus be described by [13, 14] as

$$B = \hat{i}_1 \cdot \sum_{\nu'} G_{\nu'} \cos\left(\nu'\gamma' - \varepsilon' - \varphi_0\right) \tag{1}$$

where $\gamma' = p\gamma$ is the circumferential angle, $\varepsilon' = p\varepsilon$ the mechanical angle between the d-axis and α-axis and ν' the circumferential order. The number of pole pairs is given as p. The proportionality factor $G_{\nu'}$, which describes the relationship between harmonic current and generated flux density, can be derived from [15]. The harmonic current used in [11] for compensation is an alternating fundamental current that can be described by three degrees of freedom, namely the amplitude $\hat{i}_\mathrm{k}$, the phase φ_k, and the injection direction α_k. The air-gap field caused by injecting this alternating current in the dq-reference frame can thus be described by

$$B = \hat{i}_\mathrm{k} \cos\left(k\varepsilon' + \varphi_\mathrm{k}\right) \cdot \sum_{\nu'} G_{\nu'} \cos\left(\nu'\gamma' - \varepsilon' - \alpha_\mathrm{k}\right). \tag{2}$$

The equations for calculating the resulting tensile stress waves are well known in the literature [8–10]. For this reason, their derivation is omitted here. The following Equation (3) describes the relevant radial tensile stresses resulting from Equation (2), and is correspondent with [14]:

$$\sigma_\mathrm{r} = \cdots + \frac{\hat{B}_{1,1,\mathrm{k}} \hat{B}_{1,1}}{2\mu_0} \cos\left(k\varepsilon' + \varphi_\mathrm{k}\right) \cdot \Big(\cos\left(-\alpha_\mathrm{k} + \varphi_0\right) + \cos\left(2\gamma' - 2\varepsilon' - \alpha_\mathrm{k} - \varphi_0\right)\Big). \tag{3}$$

Here, the only relevant terms are those which are independent of γ' and thus represent a force pulsation with spatial order 0.

Equation (3) has therefore shown that by injecting a harmonic current in the dq-reference frame, a force of spatial order 0 with an adjustable frequency can be generated.

Noise compensation of dual three-phase EESMs

In high power applications like energy generation in wind turbines, it is common to use multiphase electric machines. Interest in using multiphase electric machines as traction drives is also growing in the automotive industry [16]. The dual three-phase winding, often also called asymmetrical six-phase winding, is used most frequently [3]. The advantage is that limited operation is still possible despite a failure of one system or inverter. Furthermore, the use of two unconnected neutral points suppresses the zero component in the current, which in turn significantly simplifies the control of the machine.

Harmonic Currents

In addition to the advantages mentioned above, the increased number of phases also results in new degrees of freedom (DOF) that can be exploited when injecting harmonic currents. In this way, the currents in each of the two three-phase systems can be controlled independently. This makes it possible to inject an alternating fundamental current as performed in FFI, as well as to impose a phase shift of 180 between the harmonic currents of the two systems. The advantage of this strategy is that the influences of these two harmonic currents on the fundamental field in the machine cancel each other out. As a result, exclusively spatial harmonic fields are injected (HFI). This method can be illustrated with the equivalent circuit diagram of an EESM in the dq-reference frame (Fig. 1a and b). The definitions of the given parameters can be found in [17]. Fig. 1c and d also show a simplified waveform of the currents in the dq-reference frame. Here, an enlarged amplitude and an arbitrary phase angle of the harmonic current were chosen for the purposes of clarity.

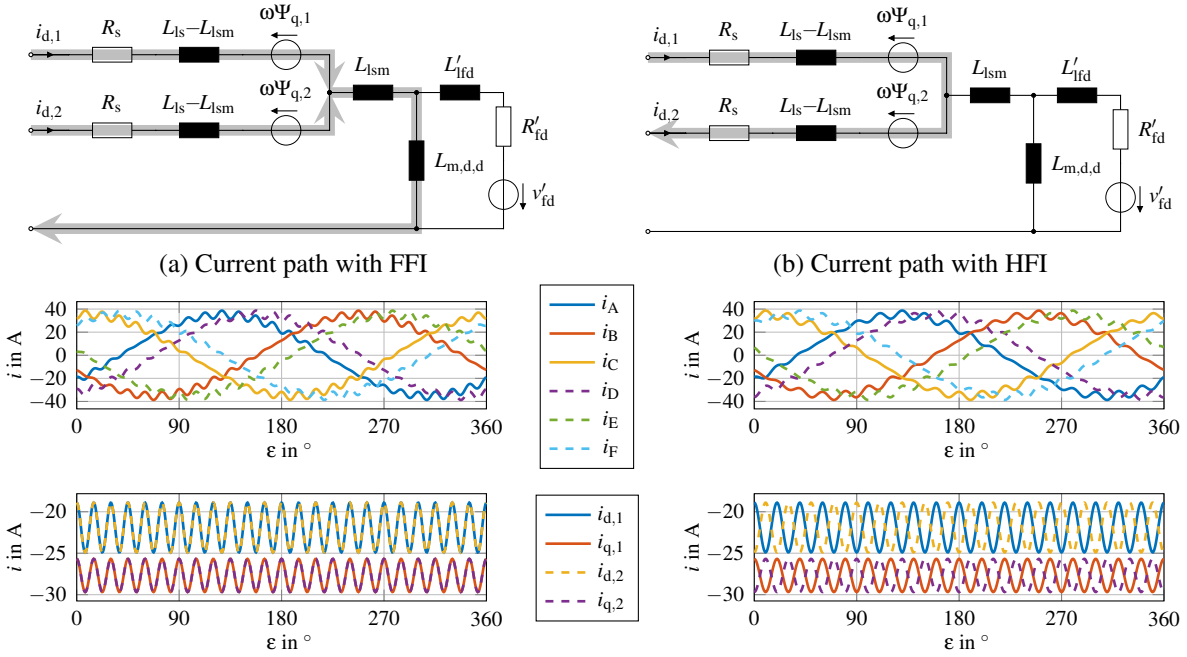

(a) Current path with FFI

(b) Current path with HFI

(c) FFI using 23rd and 25th harmonic current

(d) HFI using 17th and 19th harmonic current

Fig. 1: (a) and (b): Equivalent circuit diagram of an EESM in the dq-reference frame [17–19]. Only the d-axis is shown. (c) and (d): Waveforms of the currents in the dq-reference frame.

Stator Flux Density Harmonics

As shown in [20], dual three-phase machines do not produce the same harmonics as conventional three-phase machines. Due to the magnetic coupling between the two three-phase systems, spatial harmonics with an order which is an even multiple of six do not occur (marked as red fields in Table I). The time and spatial harmonics which do appear are marked as green fields in Table I.

The harmonics used in [11] are marked with FFI. The choice of the harmonic order was set to $k = 24$, since the machine investigated here has a mechanical resonance frequency with spatial order 0 in the tangential direction in this frequency range.

Table I: Time and spatial harmonics for dual-three phase electrical machines [3, 20].

Spatial harmonic ν'	Time harmonic $1 \pm k$								
	1	5	7	11	13	17	19	23	25
± 1								FFI	FFI
± 5							HFI		
± 7						HFI			
± 11									
± 13									

Due to the phase-opposed injection of the harmonic currents with the abbreviation HFI, there is no alternating fundamental field in the machine. Because of this, the force from the FFI method (cf.: Equation (3)) is not generated. In order to still generate a force with spatial order 0 and time order 24, the HFI method considers the interaction of the harmonics $(1 \pm k, \nu') = (-17, 7)$ and $(19, -5)$, which are marked with the abbreviation HFI, and the harmonics $(5, 5)$ and $(7, 7)$ generated by the rotor. In order to generate the desired spatial orders, two rotating currents are considered this time. The air-gap field caused by injecting the two rotating currents -17 and 19 can be described by

$$B = \hat{i}_{-17} \sum_{\nu'} G_{\nu'} \cos\left(\nu'\gamma' - (-17\varepsilon') - \alpha_{-17}\right) + \hat{i}_{19} \sum_{\nu'} G_{\nu'} \cos\left(\nu'\gamma' - 19\varepsilon' - \alpha_{19}\right). \tag{4}$$

A detailed description of the resulting rotating waves can be taken from [21]. Another way of visually representing the resulting harmonics is illustrated in Fig. 2. Here, the generated flux within the machine resulting from a sinusoidal current is shown in Fig. 2a. In Fig. 2b, it can be seen that, by injecting the harmonic currents with FFI, a field with spatial order $\nu' = p$ is created, which is also coupled to the rotor winding. In contrast, Fig. 2c indicates that the resulting fields with HFI are spatial harmonics that are not coupled or barely coupled to the rotor winding.

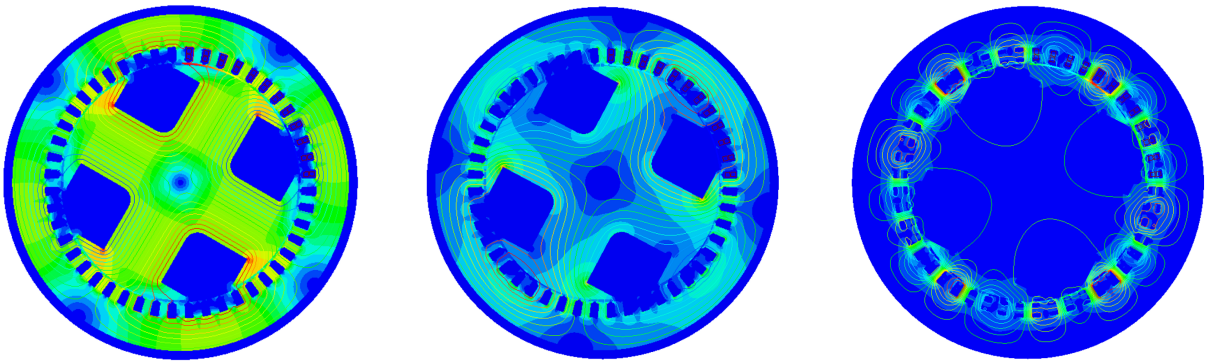

(a) Only fundamental current

(b) Only 23rd and 25th harmonic currents (FFI)

(c) Only 17th and 19th harmonic currents (HFI)

Fig. 2: Flux distribution with $I_{\mathrm{fd}} = 0\,\mathrm{A}$. Equivalent images like Fig. 2a and Fig. 2c for a PMSM can be found in [3].

Force Waves

If only the field waves with $\nu' = -5$ and $\nu' = 7$ are considered, the following spatial harmonics result from (4)

$$B = \cdots + \hat{i}_{-17} G_{7\mathrm{p}} \cos\left(7\gamma' - (-17)\varepsilon' - \alpha_{-17}\right) + \hat{i}_{19} G_{-5\mathrm{p}} \cos\left(-5\gamma' - 19\varepsilon' - \alpha_{19}\right). \tag{5}$$

Together with the rotor hamonics

$$B_{5,5} = \hat{B}_{5,5} \cos\left(5\gamma' - 5\varepsilon' - \varphi_{5,5}\right) \text{ and } B_{7,7} = \hat{B}_{7,7} \cos\left(7\gamma' - 7\varepsilon' - \varphi_{7,7}\right) \tag{6}$$

Table II: Operating point investigated

S_N	$17.3\,\mathrm{kV\,A}$
$I_\mathrm{d,N}$	$-21.93\,\mathrm{A}$
$I_\mathrm{q,N}$	$-27.68\,\mathrm{A}$
I_fd	$22.08\,\mathrm{A}$
p	2
$\lvert\underline{\sigma}_\mathrm{n,0}\rvert$	$226.2\,\mathrm{N\,m^{-2}}$
$\lvert\underline{\sigma}_\mathrm{t,0}\rvert$	$214.5\,\mathrm{N\,m^{-2}}$

Table III: Currents required to compensate for the radial and tangential modes 0

FFI		HFI	
$\hat{i}_{-23}$	$0.425\,\mathrm{A}$	$\hat{i}_{-17}$	$40.7\,\mathrm{A}$
$\hat{i}_{25}$	$0.302\,\mathrm{A}$	$\hat{i}_{19}$	$13.12\,\mathrm{A}$
$\lvert\underline{\sigma}^*_\mathrm{n,0}\rvert$	$0.887\,\mathrm{N\,m^{-2}}$	$\lvert\underline{\sigma}^*_\mathrm{n,0}\rvert$	$0.526\,\mathrm{N\,m^{-2}}$
$\lvert\underline{\sigma}^*_\mathrm{t,0}\rvert$	$0.464\,\mathrm{N\,m^{-2}}$	$\lvert\underline{\sigma}^*_\mathrm{t,0}\rvert$	$0.028\,\mathrm{N\,m^{-2}}$

the relevant terms of the tensile stress are:

$$\sigma_\mathrm{r} = \cdots + \frac{1}{2\mu_0}\left(\hat{i}_{19} G_{-5\mathrm{p}} \hat{B}_{5,5} \cos\left(-24\varepsilon' - \varphi_{5,5} - \alpha_{19}\right) + \hat{i}_{-17} G_{7\mathrm{p}} \hat{B}_{7,7} \cos\left(24\varepsilon' + \varphi_{7,7} - \alpha_{-17}\right)\right). \quad (7)$$

The same approach can be applied to the tangential force. However, the analytical calculation of the tangential force is outside the focus of the paper. The difference between FFI and HFI can also be demonstrated with the help of the force equation. If (7) is compared with (2), it can be seen that, in contrast to [11], two tensile stresses with the same frequency arise. The amplitude of the tensile stress can be influenced by the amplitude of the harmonic currents and their phase by the choice of the injection direction.

Comparison of the currents required by FFI and HFI

This section presents the calculation of the compensation currents needed to produce a change in the tensile stress by the value $\Delta\underline{\sigma}$. These calculations were carried out with the help of FEM simulations. From (7), it is clear that the relationship between current and tensile stress can be described by a complex factor. With reference to [11], this factor will be called $\underline{\eta}$. The change in the tensile stress in the radial direction $\Delta\underline{\sigma}_\mathrm{n}$ caused by the complex harmonic current from [3] can consequently be described by

$$\Delta\underline{\sigma}_\mathrm{n} = \underline{\eta}_{\mathrm{n},-17} \cdot \underline{i}_{-17} + \underline{\eta}_{\mathrm{n},19} \cdot \underline{i}_{19}. \quad (8)$$

Considering the tangential forces, this equation expands into the matrix notation

$$\begin{bmatrix} \Delta\underline{\sigma}_\mathrm{n} \\ \Delta\underline{\sigma}_\mathrm{t} \end{bmatrix} = \begin{bmatrix} \underline{\eta}_{\mathrm{n},-17} & \underline{\eta}_{\mathrm{n},19} \\ \underline{\eta}_{\mathrm{t},-17} & \underline{\eta}_{\mathrm{t},19} \end{bmatrix} \begin{bmatrix} \underline{i}_{-17} \\ \underline{i}_{19} \end{bmatrix}. \quad (9)$$

With the condition that the determinant of the matrix is not equal to zero, the matrix can be inverted. This leads to the relationship between the complex harmonic currents and the tensile stress, which can be described by

$$\begin{bmatrix} \underline{i}_{-17} \\ \underline{i}_{19} \end{bmatrix} = \begin{bmatrix} \underline{\eta}_{\mathrm{n},-17} & \underline{\eta}_{\mathrm{n},19} \\ \underline{\eta}_{\mathrm{t},-17} & \underline{\eta}_{\mathrm{t},19} \end{bmatrix}^{-1} \begin{bmatrix} \Delta\underline{\sigma}_\mathrm{n} \\ \Delta\underline{\sigma}_\mathrm{t} \end{bmatrix}. \quad (10)$$

A determinant of nonzero also shows that the radial and tangential spatial directions are linearly independent and can therefore be compensated independently. With an algorithm similar to the one developed in [14], the complex parameters $\underline{\eta}$ from (10) can be identified using FEM simulations. This makes it possible to calculate the right harmonic currents to compensate for a given tensile stress. The calculations are performed iteratively as described in [14]. This gives the possibility to compensate for nonlinearities and inaccuracies of the determination of the complex parameters.

The calculation was carried out for a salient-pole EESM. Data concerning the machine and the tensile stresses to be compensated can be found in Table II. The results of the compensation current calculation are shown in Table III. These show that harmonic currents of $\hat{i}_{-23} = 0.435\,\mathrm{A}$ and $\hat{i}_{25} = 0.302\,\mathrm{A}$ are required to reduce the radial and tangential tensile stresses to below 1 % using the FFI method. These fig-

ures correspond to 1.2 % and 0.9 % of the fundamental amplitude, respectively, so no significant effects on the winding losses are expected.

Compensation employing the HFI method means that significantly higher harmonic amplitudes are required to similarly reduce the radial and tangential tensile stresses to around 1 %. This requires $\hat{i}_{-17} = 40.7\,\mathrm{A}$ and $\hat{i}_{19} = 13.12\,\mathrm{A}$. These figures correspond to 115 % and 37.2 % of the fundamental amplitude, respectively, and are thus of the same order of magnitude as the fundamental amplitude. The high compensation currents can be explained, for instance, by the chorded winding in the machine. Since the fields with a spatial order of -5 and 7 are suppressed, significantly higher compensation currents are required for the HFI method.

In order to evaluate the compensation methods, their influence on the losses within the machine is of crucial importance. The iron losses within the machine increase by 2 % with the FFI method. The HFI method increases the iron losses by 4 %. These numbers were determined by means of an FEM simulation. There is a more significant effect on the winding losses in the stator. Here, the losses increase by 200 % with the HFI method. With the FFI method, the winding losses increase by just 0.2 %. This leads to the conclusion that the FFI method is to be preferred for efficiency-optimized operation of the EESM.

Parasitic Effects

In addition to the desired change in the radial and tangential tensile stresses with spatial order 0, a number of unwanted parasitic effects arise from injecting the harmonic currents. Due to the alternating fundamental field of the FFI method (see Fig. 3), a voltage with k times the fundamental frequency is induced into the field winding (see Fig. 4). Since there is no alternating fundamental field with HFI, the induced voltage is considerably lower than with the FFI method. Still, regular operation with sinusoidal currents exhibits even smaller induced voltages.

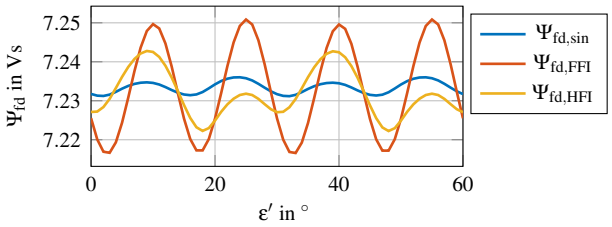

Fig. 3: Rotor flux linkage

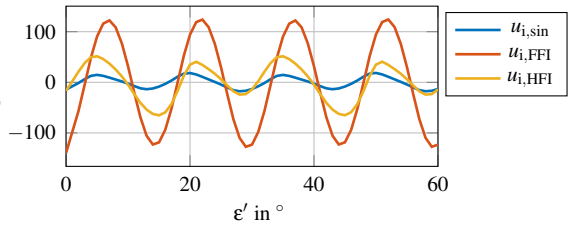

Fig. 4: Induced voltage in the field winding

Typical voltage supplies for a field winding are not able to compensate for the induced voltage. For this reason, a harmonic current will flow in the rotor, which, according to Lenz's law, will counteract the alternating fundamental field. To investigate the influence of this effect on the calculation of the harmonic currents, FEM simulations with voltage injection into the field winding were also performed. It can be seen in Fig. 6 that a harmonic current of $\hat{i}_{\mathrm{fd},24} = 0.25\,\mathrm{A}$ with a frequency of $f_{\mathrm{fd},24} = 24 \cdot f_1$ flows through the field winding and thus changes the rotor flux linkage (see Fig. 5). This increases the harmonic currents required for FFI compensation to $\hat{i}_{-23} = 0.624\,\mathrm{A}$ and $\hat{i}_{25} = 0.449\,\mathrm{A}$. These are increases of 46.8 % and 48.7 %, respectively. Fig. 5 and Fig. 6 also show that the influence of the HFI method on the rotor is lower than that of the FFI method. The required compensation currents change by 23 % and −38 % to become $\hat{i}_{-17} = 50.1\,\mathrm{A}$ and $\hat{i}_{19} = 8.1\,\mathrm{A}$, respectively. The effects of an pulsating excitation current on the force excitation and also on the induced voltage in the stator has also been demonstrated in [5].

In addition, the harmonic currents in the stator cause new tensile stresses which were not considered in the derivation. For FFI, this includes the spatial order $2p$ with the harmonic orders 2 ± 24 (see Fig. 7). A reduction in the tensile stress waves is shown in green and an increase in red. Fig. 8 shows the force changes resulting from the HFI method. The changes in the parasitic forces are significantly larger for HFI than for FFI, due to the significantly higher current amplitude needed for compensation. The parasitic forces primarily arise from the interaction between the additional spatial harmonic fields and the fundamental field.

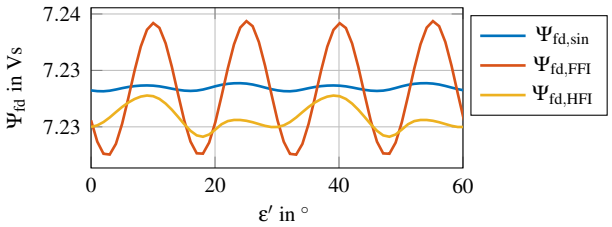

Fig. 5: Rotor flux linkage with voltage injection

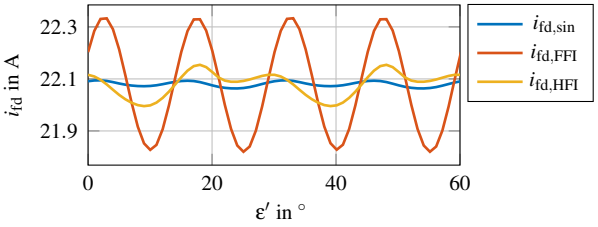

Fig. 6: Current in the field winding with voltage injection

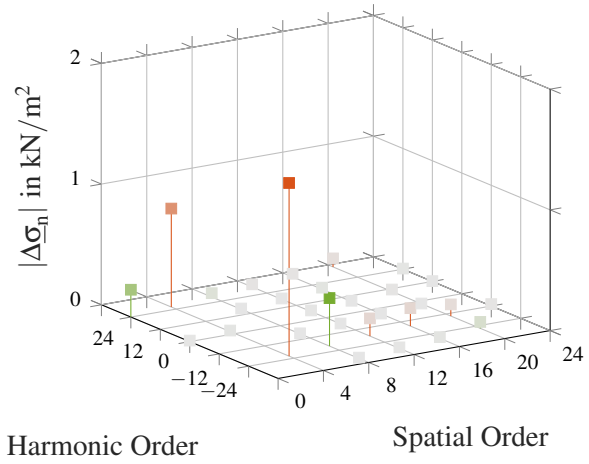

Fig. 7: Changes in the tensile stress with FFI

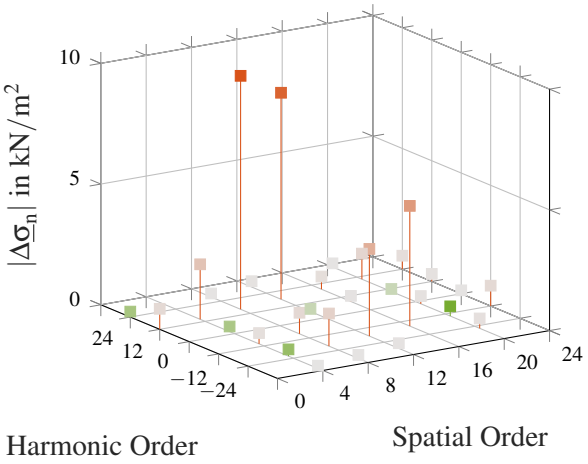

Fig. 8: Changes in the tensile stress with HFI

Conclusion

This paper provides an extensive comparison between two methods known from the literature for noise suppression in dual three-phase EESMs: fundamental field injection (FFI) and harmonic field injection (HFI). For HFI, the analytical prediction of harmonic currents, which has already been demonstrated for FFI, was adapted. Using FEM calculations, it is shown that compensation of the radial and tangential tensile stresses of mode 0 can be achieved with both FFI and HFI. FFI compensation requires significantly lower harmonic current amplitudes and thus also causes considerably lower winding losses than HFI compensation. In addition, it can be seen that with FFI, a voltage is induced into the field winding by the alternating fundamental field. Therefore, a harmonic field current controller with sufficient voltage reserve is essential to prevent harmonic currents from flowing in the field winding. If suitable harmonic current controllers are not available, it is shown in this paper that the required harmonic currents in the stator become significantly larger. Future research will analyze whether the selection of the compensation method depending on the operating point is advisable.

References

[1] J. Redlich, J. Juergens, K. Brune, and B. Ponick, "Synchronous machines with very high torque density for automotive traction applications," in *2017 IEEE International Electric Machines and Drives Conference (IEMDC)*, 2017, pp. 1–8.

[2] A. Hofmann, F. Qi, T. Lange, and R. W. De Doncker, "The breathing mode-shape 0: Is it the main acoustic issue in the pmsms of today's electric vehicles?" in *2014 17th International Conference on Electrical Machines and Systems (ICEMS)*, 2014, pp. 3067–3073.

[3] P. Hollstegge, A. Wanke, and R. W. De Doncker, "Noise mitigation in dual three-phase internal permanent magnet machines by injection of current harmonics," in *The Journal of Engineering*, vol. 2019, no. 17. IET, 2019, pp. 4273–4277.

[4] M. Harries, M. Hensgens, and R. W. De Doncker, "Noise reduction via harmonic current injection for concentrated-winding permanent magnet synchronous machines," in *2018 21st International Conference on Electrical Machines and Systems (ICEMS)*, 2018, pp. 1157–1162.

[5] F. Evestedt, J. J. Pérez-Loya, C. J. D. Abrahamsson, and U. Lundin, "Controlling airgap magnetic flux density harmonics in synchronous machines using field current injection," *Electrical Engineering*, vol. 103, no. 1, pp. 195–203, 2021.

[6] J. Nägelkrämer, A. Heitmann, and N. Parspour, "Application of dynamic programming for active noise reduction of pmsm by reducing torque ripple and radial force harmonics," in *2018 AEIT International Annual Conference*, 2018, pp. 1–6.

[7] S. Ciceo, F. Chauvicourt, J. Gyselinck, and C. Martis, "PMSM current shaping for minimum joule losses while reducing torque ripple and vibrations," *IEEE Access*, vol. 9, pp. 114 705–114 714, 2021.

[8] B. Cassoret, R. Corton, D. Roger, and J.-F. Brudny, "Magnetic noise reduction of induction machines," *IEEE Transactions on Power Electronics*, vol. 18, no. 2, pp. 570–579, 2003.

[9] D. Belkhayat, D. Roger, and J. F. Brudny, "Active reduction of magnetic noise in asynchronous machine controlled by stator current harmonics," *IET Conference Proceedings*, pp. 400–405(5), 1997, publisher: Institution of Engineering and Technology.

[10] D. Franck, M. van der Giet, and K. Hameyer, "Active reduction of audible noise exciting radial force-density waves in induction motors," in *2011 IEEE International Electric Machines Drives Conference (IEMDC)*, 2011, pp. 1213–1218.

[11] J. Andresen, S. Vip, A. Mertens, and S. Paulus, "Theory of influencing the breathing mode and torque pulsations of permanent magnet electric machines with harmonic currents," in *2020 22nd European Conference on Power Electronics and Applications (EPE'20 ECCE Europe)*, 2020, pp. P.1–P.9.

[12] J. Andresen, S. Vip, A. Mertens, and S. Paulus, "Compensation of the radial and circumferential mode 0 vibration of a permanent magnet electric machine based on an experimental characterisation," in *2020 22nd European Conference on Power Electronics and Applications (EPE'20 ECCE Europe)*, 2020, pp. P.1–P.9.

[13] G. Müller and B. Ponick, *Theorie elektrischer Maschinen*, 6th ed., ser. Elektrische Maschinen. Weinheim: Wiley-VCH, 2009, no. 3.

[14] J. Andresen, "Aktive Geräuschunterdrückung in einer permanentmagneterregten Synchronmaschine mit Hilfe von Stromoberschwingungen," Dissertation, Faculty of Electrical Engineering and Computer Science, Leibniz University Hannover, Germany, 2021.

[15] J. F. Gieras, J. C. Lai, and C. Wang, *Noise of polyphase electric motors*, ser. Electrical and computer engineering. Boca Raton, FL: CRC/Taylor & Francis, 2006, no. 129.

[16] A. Salem and M. Narimani, "A review on multiphase drives for automotive traction applications," *IEEE Transactions on Transportation Electrification*, vol. 5, no. 4, pp. 1329–1348, 2019.

[17] R. F. Schiferl and C. M. Ong, "Six phase synchronous machine with ac and dc stator connections, part i: Equivalent circuit representation and steady-state analysis," *IEEE Transactions on Power Apparatus and Systems*, vol. PAS-102, no. 8, pp. 2685–2693, 1983.

[18] S. Gradev, J. Reuss, and H.-G. Herzog, "A general voltage-behind-reactance formulation of a multivoltage n 3-phase hybrid-excited synchronous machine," *IEEE Transactions on Energy Conversion*, vol. 31, no. 4, pp. 1452–1461, 2016.

[19] J. Heseding, "Baukastensysteme für den Antriebsstrang von Elektrofahrzeugen," Dissertation, Faculty of Electrical Engineering and Computer Science, Leibniz University Hannover, Germany, 2018.

[20] D. G. Dorrell, C. Y. Leong, and R. A. McMahon, "Analysis and performance assessment of six-pulse inverter-fed three-phase and six-phase induction machines," *IEEE Transactions on Industry Applications*, vol. 42, no. 6, pp. 1487–1495, 2006.

[21] P. Hollstegge, "Injektion raumzeigerzerlegter Stromharmonischer zur Minderung tonaler Geräuschanteile in asymmetrisch sechsphasigen Permanentmagnetsynchronmaschinen," Dissertation, Faculty of Electrical Engineering and Information Technology, RWTH Aachen University, Germany, 2021.